JOURNAL OF Materials CHEMISTRY

Carbon anode materials based on melamine resin

Yuping Wu,*[a,b] Shibi Fang[b] and Yingyan Jiang[b]

[a] *Tsinghua University, Beijing 102201, China. E-mail: hyy200@tsinghua.edu.cn*
[b] *Institute of Chemistry, Chinese Academy of Sciences, Beijing 100080, China*

Received 1st July 1998, Accepted 1st July 1998

We have obtained carbon anode materials based on a melamine resin. Through elemental analysis, X-ray powder diffraction, BET measurement and X-ray photoelectron spectroscopy, the effects of heat-treatment temperature and doping of phosphorus were investigated. Temperature affects mainly the nitrogen content, the size of graphite crystallites and the number of micropores in the carbons, and thus their reversible capacity changes with temperature. The highest reversible capacity occurs at 600 °C. The addition of phosphoric acid can affect the carbon structure and relative content of graphene nitrogen. Its behaviour changes with temperature. Only at high temperature, can the doped phosphorus favour the enhancement of reversible capacity.

Anode materials for lithium secondary batteries have been studied widely since their commercialization in 1991. Recently, novel anode materials such as $Li_xM_{3-x}N$ (M = transition metal)[1,2] and tin-based composite oxides[3,4] have been reported, and offer high reversible capacity compared with carbon-based materials. However, the preparation of $Li_xM_{3-x}N$ is critical for commercialization. While tin composite oxide is suggested to react irreversibly with lithium to form Li_2O,[4] and the contribution to reversible capacity is regarded to arise from the formation of an alloy of lithium with the reduced tin, the alloy has long been regarded as unsatisfactory for use as an anode material for lithium rechargeable batteries for long cycle use. Thus, the availability of novel anode materials for practical use is still in doubt.

As the lithium-ion battery has many advantages over traditional rechargeable batteries such as the lead acid, Ni–Cd and Ni–MH, it is regarded as potentially an ideal power source for electrical vehicles. However, electric vehicles require fast charge and discharge properties,[5] *i.e.* good conduction within the cell. From this viewpoint, the best candidate in the long run may be carbon-based materials.

Recently, carbon anode materials doped with heteroatoms such as boron,[6] silicon,[7] nitrogen[8–10] and transition metals[11–13] have been reported. Some of these have achieved some success. For example, the doping of nitrogen favours the enhancement of reversible lithium capacity when it is bonded satisfactorily.[10] In carbons, nitrogen exists in three states: as graphene nitrogen, conjugated nitrogen and amine-group nitrogen. The first is the main cause of the observed enhancement of reversible capacity while the third is the cause of increase of irreversible capacity. In polymeric carbons, N ls XPS spectra indicate that nitrogen appears only as graphene nitrogen and conjugated nitrogen. Melamine resin is a commercially available and very cheap cross-linked polymer, and is perhaps an attractive precursor for anode materials. Furthermore, as far as we know, there are no reports about the effects of specific heat-treatments on the properties of the derived carbon. Here, we study the effects of temperature on chemical and electrochemical properties of the prepared carbons based on this type of precursor.

It is also reported that phosphorus in carbonaceous materials can enhance their capacity for lithium intercalation[14,15] and the effect of phosphorus varies with different precursor and treatment. Omura *et al.* added phosphorus to polyfurfuryl alcohol and then heated the mixture to 1200 °C to form phosphorus-doped carbon. The enhancement of reversible capacity is attributed to the dopant phosphorus, *i.e.* the $(C_6H_5O)_2P(=O)OH$ formed.[14] Tran *et al.* dried a slurry of petroleum coke and concentrated H_3PO_4 in an acetone solution at room temperature and heat-treated the dry material at 1050 °C to obtain a phosphorus-doped carbon. In this case, the increase of reversible capacity is regarded as due to facilitation of lithium intercalation by the expansion of the layer spacing at the edge of the carbon structure.[15] Here we present also the effects of added phosphorus on carbons based upon melamine resin and find it differs from that reported elsewhere.

Experimental

Preparation of carbon materials

Melamine resin was synthesized from melamine and formaldehyde (molar ratio 1:2) at pH = 9.0. A thin film of the resin was put into a tube furnace, soaked at 250 °C for 4 h, and later pyrolyzed under an argon atmosphere at different temperatures from 400–900 °C, and the product was powdered through 320 mesh sieve. Analysis of physicochemical properties proceeded with the carbon powder obtained.

The introduction of phosphorus was different from that reported.[14,15] The melamine resin obtained was powdered and mixed with varying amounts of concentrated H_3PO_4 for 20 min in a ball mill, then the mixture was heat-treated at 100 °C for 4 h. During this period, H_3PO_4 reacts with the hydroxyl and amine groups in the melamine resin, and thus phosphorus was incorporated into the polymer structure. The treated mixture was then pyrolyzed in the above tube furnace under an argon atmosphere. The carbon product was also powdered to pass a 320 mesh. The amount of H_3PO_4 added was based on the weight of melamine resin.

Analysis of carbon material

Elemental analysis was carried out by the Heratus CHN-rapid method. X-Ray powder diffraction (XRD) was carried out using a D/MAX-3B diffractometer. X-Ray photoelectron spectra (XPS) were obtained using an ES300 (Kratos). The measurement of specific surface area and micropore size distribution was done using a Sorpmatic 1800 instrument. The surface area results obtained were based on the Brunauer, Emmett and Teller (BET) equation. Thermogravimetric analysis was performed using a Perkin-Elmer Thermal Analysis System, 7, under a high purity argon atmosphere. The heating rate was 20 °C min^{-1} and there was no soak time in the process, different from the above mentioned heat-treatment.

Measurement of capacity

By pressing the mixture of the carbon powder obtained with 5% PTFE powder as a binder into a thin film, pellets of this with diameter 1 cm and weight *ca.* 10 mg were cut off and used as working electrodes. Before placing into a glove box filled with argon and free of water and oxygen, the electrodes were weighed precisely and dried overnight at 120 °C under vacuum. Coin-type test cells were constructed from these electrode pellets, using porous polypropylene as separator and lithium foil as counter and reference electrode. The electrolyte used was a 1 M solution of $LiClO_4$ dissolved in a mixture of 30% ethylene carbonate and 70% diethyl carbonate by volume. The cells were discharged and charged in the voltage range −0.03 to 2.0 V *vs.* Li/Li^+ at a constant current of 0.2 mA, using a computer-controlled constant current cycler. The cut-off voltage of discharge was selected at −0.03 V because there was an overpotential resulting from internal resistance.[12]

Results and discussion

Effect of temperature on the carbons from the melamine resin

Table 1 shows the results of elemental analysis of the samples. The H/C and N/C atomic ratios decrease monotonically with the heat-treatment temperature, and the sample eventually approaches pure carbon. When the temperature is low, the nitrogen content of sample A301 is near to that of the precursor A300. This indicates the carbonization degree is very low and the main reaction is the dehydration of the polymer. Table 1 also gives the product yield for the carbon samples as a percentage of the starting weight of the melamine resin.

Fig. 1 shows the X-ray powder diffraction pattern of the polymeric carbons from the different heat-treatment temperatures and some of the results are summarized in Table 1. Only the diffraction peak of 002 planes can be identified, indicating

Table 1 Results of elemental analysis and X-ray powder diffraction of the carbons prepared at different temperatures from melamine resin

Sample	Temperature/ °C	Yield (wt.%)	N/C	H/C	d_{002}/Å	L_c/Å[a]
A300	20	100	1.190	0.962	—	—
A301	400	63.4	0.930	0.480	3.338	20.7
A302	500	50.2	0.570	0.377	—	—
A303	600	43.1	0.217	0.241	3.434	12.22
A304	700	35.0	0.124	0.187	3.419	13.25
A305	800	25.8	0.067	<0.03	3.411	14.23
A306	900	15.1	0.043	<0.03	3.403	15.72

[a] $L_c = k\lambda/\beta\cos\theta$ (k: shape factor, as to amorphous carbon, 0.9).[16]

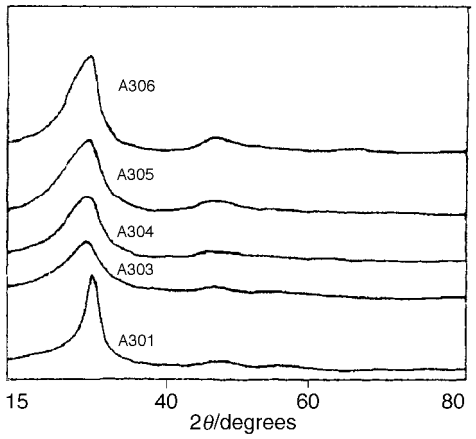

Fig. 1 X-Ray diffraction pattern of carbons prepared at different heat treatments.

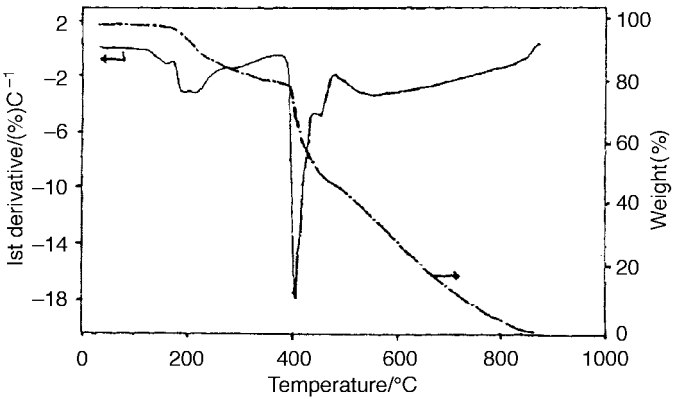

Fig. 2 Thermogravimetric curve for melamine resin(1:2).

that this kind of carbon is largely amorphous and consists of graphite crystallites and disordered areas. However, the inter-layer-spacing d_{002} is very small, around 3.4 Å, perhaps due to the high content of nitrogen and the fact that the diameter of N(1.50 Å) is smaller than that of C(1.54 Å). The crystallite size along the c axis L_c increases with temperature above 600 °C.

Fig. 2 shows the results from thermogravimetric analysis (TGA) and suggests the possible reactions that may take place during the carbonization. Melamine resin does not begin to carbonize until 400 °C and below this temperature the main reaction is dehydration. As shown in Fig. 1, the 002 peak of sample A301 is sharper than that of the others. The main cause of this may be due to the incomplete carbonization. In the melamine resin, the charge distribution of the C_3N_3 six-membered ring is not homogeneous with N slightly positive and C slightly negative; there is a strong interaction between the six-membered rings and thus the interlayer distance is very small, close to that of graphite 3.354 Å, and the stacking of the rings is more ordered than in the other carbons prepared at higher temperature. The same behaviour is also observed for a phenol–formaldehyde resin.[17] While Fig. 2 suggests that the yield for carbon at high temperature will be very low the actual yield is higher (Table 1). This is because that we additionally soaked the melamine–formaldehyde resin at 250 °C for 4 h. In the absence of this additional treatment the carbon yield was very low.

Fig. 3 shows the distribution of micropores of the carbons prepared at different temperatures and shows that the distribution of micropores is not the same as reported following X-ray small angle scattering(SAXS),[18] which indicates the distribution of pores is almost identical. The present data indicate that the micropores are divided mainly into three size ranges: 1.1, 1.9 and 3.5 or 6.1 nm. The lowest size corresponds to vacancies left by the release of small molecules. With increase of temperature, more small molecules are released, and more micropores of diameter 1.1 and 1.9 nm are produced. At the same time, the small micropores can coalesce and form larger pores during the heat-treatment,[19] therefore the size of the third group of micropores changes from 3.5 nm (600 °C) to 6.1 nm (800 °C).

Fig. 4 shows the specific surface area of the carbons obtained. At low temperature (Fig. 2), a carbon skeleton is not formed, and the vacancies left by the release of small molecules such as H_2O can not be retained. Consequently, the number of micropores is very small. When the temperature is increased above the carbonization temperature, the vacancies left can be retained giving rise to an increase in specific surface area. As mentioned above, the small micropores can coalesce and form larger pores, and some are so large that they can not be regarded as micropores, and could not be detected by

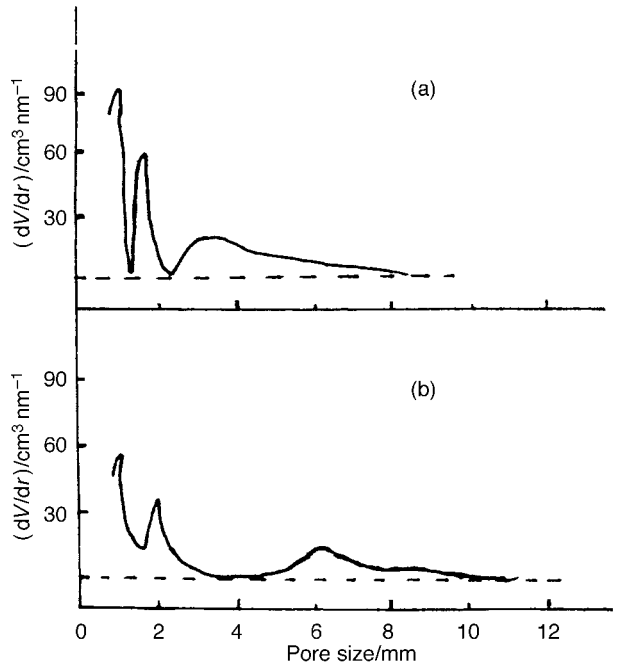

Fig. 3 Distribution of micropores of carbons heat treated at different temperatures: (a) A303, (b) A305.

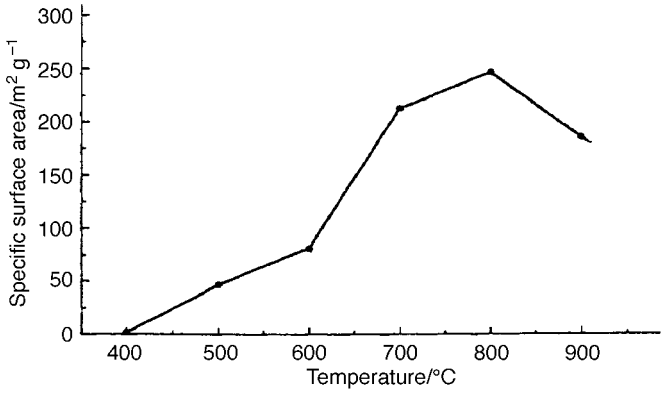

Fig. 4 Change of specific BET surface area for carbons from different heat treatments.

BET, thus a maximum in the number of micropores will be present, behaviour consistent with that reported previously.[20]

Fig. 5 shows the charging profiles of the carbons produced at different temperatures. The reversible capacity initially increases with temperature, and reaches a peak at 600 °C, and then decreases above this temperature.

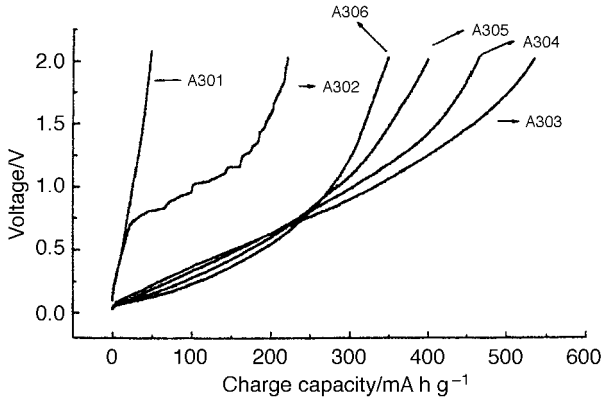

Fig. 5 Charging curves of different carbon anodes.

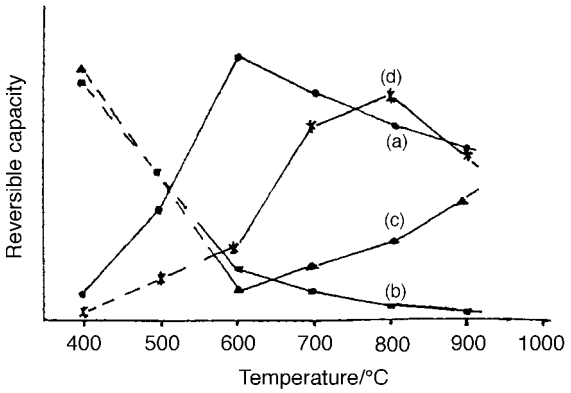

Fig. 6 Effect upon reversible capacity of nitrogen (b), size of graphite crystallites (c), micropores (d) and total results (a).

As reported previously,[10] the nitrogen in polymeric carbon can affect the reversible capacity; the higher the content of nitrogen, the higher the reversible capacity. Moreover, graphite crystallites can also accommodate lithium *via* the traditional graphite intercalation compound mechanism;[17] the larger their size, the more lithium can be intercalated. In addition, the nanoscopic pores or micropores can act as 'reservoirs' for lithium storage.[18,21] From our results above, the heat-treatment temperature affects these three factors, and the effects of these factors on the reversible capacity of the carbon is illustrated schematically in Fig. 6(b)–(d). It must be noted that, because of the action of nitrogen, micropores can not act effectively below 400 °C because the carbon structure is not yet formed, (shown as dashed lines). The total effect is represented in Fig. 6(a). If there is no nitrogen, then the maximum of reversible capacity will be located, at high temperature (700 °C), as reported previously.[17]

As to carbons obtained between 1000 and 2000 °C, from our above discussion, it can be appreciated why their reversible capacity is the lowest among carbons prepared between 500 and 3000 °C.[18] The number of micropores is very small for this type of amorphous carbon (prepared by heat-treatment at temperatures below 1000 °C) and the size of graphite crystallites is very small compared with that of graphite or graphitized carbon (prepared from heat-treatment at temperatures above 2000 °C).

As to the action of hydrogen, direct interaction between lithium atoms and the peripheral C—H bonds has been suggested based on the linear relationship between reversible

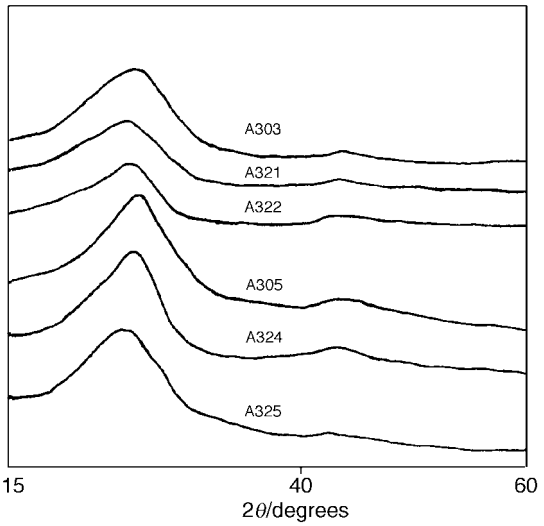

Fig. 7 X-Ray powder diffraction patterns of carbons and phosphorus doped carbons.

Table 2 Results of elemental analysis, X-ray powder diffraction and X-ray photoelectron spectroscopy of the carbons doped with and without phosphorus

Sample	Temperature/°C	Amount of added H_3PO_4 (wt.%)	d_{002}/Å	N/C	Relative content (%)	
					Graphene N	Conjugated N
A303	600	0	3.434	0.217	50.6	49.4
A321	600	5.0	3.506	0.214	—	—
A322	600	10.0	3.615	0.213	61.8	39.2
A305	800	0	3.411	0.067	—	—
A324	800	5.0	3.506	0.065	—	—
A325	800	10.0	3.575	0.065	—	—

capacity and the H/C atomic ratio.[22,23] However, from ^{7}Li NMR and ^{1}H decoupling measurements,[24] no significant change in the ^{7}Li NMR was seen suggesting that there are no H nuclei around Li and no direct interaction between Li and H. In other words, the action of hydrogen on the reversible capacity is not clear. In fact, carbon with a H/C ratio as low as 0.027 can have a very large reversible capacity.[21] Thus, in Fig. 6, we did not take the effect of H into account.

Effects of phosphorus introduction on the properties of the carbon anode

In the melamine resin, groups such as —OH, —NH_2 and —NH— can react with phosphoric acid. By the introduction of phosphoric acid, we can effectively incorporate phosphorus into the carbon structure.

Fig. 7 shows the X-ray powder diffraction pattern of carbons doped with and without phosphorus, and some results are summarized in Table 2. All the d_{002} interlayer spacings are enlarged after doping with phosphorus, the width of the 002 peaks broadens at 600 °C which alters little at 800 °C. This indicates that the doping of phosphorus is unfavorable for the formation of the carbon structure or growth of graphite crystallites at low temperatures, and the effect of the doped phosphorus on the growth of graphite crystallites is not significant at high temperature.

Table 2 shows the results of elemental analysis of carbons doped with and without phosphorus. Although the introduction of phosphoric acid results in a decrease of nitrogen content, this effect is not large.

Fig. 8 presents the comparison of X-ray photoelectron spectra in the N ls region in carbons prepared at 600 °C with and without phosphorus doping, and the results are summarized in Table 2. The binding energy peaks at 398.5 and 400.2 eV are attributed to graphene nitrogen and conjugated nitrogen, respectively.[10] The comparison illustrates that the relative content of graphene nitrogen is increased and that of conjugated nitrogen is decreased after doping with phosphorus. In melamine resin, there are two types of nitrogen, those in C_3N_3 six-membered rings and the others at the side of the ring. The former can be incorporated more easily into the carbon structure as graphene nitrogen while the latter can be incorporated more easily into the carbon structure as conjugated nitrogen, and can also react more readily with phosphoric acid

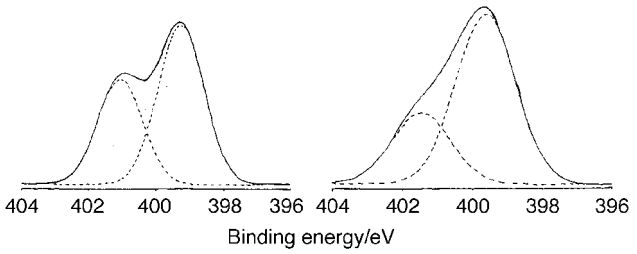

Fig. 8 N 1s binding energy spectra of carbons heat treated at 600 °C: (a) A303, (b) A325.

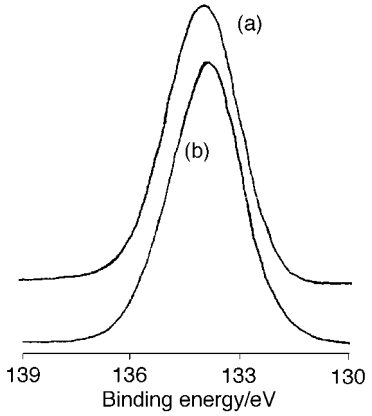

Fig. 9 Binding energy spectra of P 2p for carbons heat treated at (a) 600 °C (A303) and (b) 800 °C (A325).

and escape from the carbon as gases such as NH_3 during heat-treatment, thus lowering the relative content of conjugated nitrogen. At 800 °C, the effect of phosphorus addition is the same.

Fig. 9 shows the binding energy spectra in the P 2p region in carbons prepared at different temperatures. The binding energy peaks situated at 133.80 and 133.76 eV correspond to that of phosphorus in carbons prepared at 600 and 800 °C, respectively. This indicates that the phosphorus atom bonds not only with carbon but also with oxygen. The doped phosphorus is present as C—P—O in the carbons, as suggested by Omura *et al.* for $(C_6H_5)_2P(=O)OH$.[14] Other studies also suggest that P—O species are likely to be present after the impregnation of carbon with a phosphorus compound and subsequent heat-treatment.[25,26] At high temperature, the doped phosphorus bonds with the carbon structure slightly more strongly, consistent with the results from X-ray powder diffraction as described above.

Fig. 10 and 11 show the charging profiles of carbons with and without doped phosphorus. At 600 °C, the doping gives rise to a decrease of reversible capacity, the main decrease

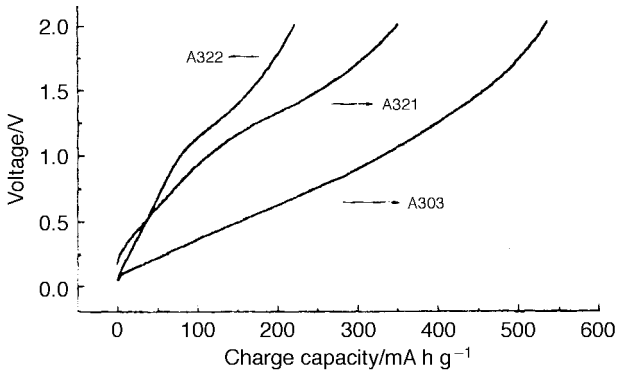

Fig. 10 Charging curves of carbons heat treated at 600 °C.

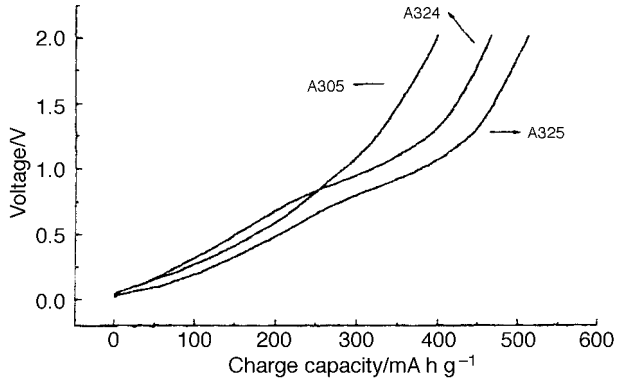

Fig. 11 Charging curves of carbons heat treated at 800 °C.

being below 0.9 V. At 800 °C, the doped phosphorus results in the enhancement of reversible capacity, and the main enhancement is above 0.9 V.

From the results obtained, the phosphorus exists in the carbon structure as C—P—O, and is present not only at edge-plane sites[15] but also in the carbon bulk as dopant.[14] The atomic diameter of phosphorus (2.12 Å) is larger than that of carbon (1.54 Å), thus the doped phosphorus expands not only the layer planes at the surface of the particle but also the interlayer spacing in the graphite crystallites as measured by X-ray diffraction. Consequently, the doped phosphorus will facilitate the intercalation of lithium. However, as illustrated above, the doped phosphorus behaves differently according to the heat-treatment temperature. A possible reason is due to its different effects on the carbon structure. At 600 °C, the growth of graphite crystallites is unfavorable while at 800 °C there is not much difference in the growth of graphite crystallites relative to undoped samples. Fig. 11 also shows a slight indication of a plateau near 0.9 V in the charging curves for the phosphorus-doped carbons. Although a similar plateau has also been observed and reported elsewhere,[15] it is more evident here.

From the above, favourable doping of phosphorus does not significantly lower the degree of carbonization and only at temperatures above 600 °C can this effect be realized and is why doping of phosphorus was reported previously to proceed at 1200 and 1050 °C.[14,15]

Conclusion

The work presented here shows that carbons based on melamine resin can have a large reversible capacity for lithium insertion. The effects of heat-treatment temperature on the properties of the carbon were studied by elemental analysis, X-ray powder diffraction and BET measurements. The heat-treatment temperature mainly affects the nitrogen content, the size of graphite crystallites and the number of micropores. All of these factors result in the total reversible capacity being initially increased with temperature and then decreased. At 600 °C, the reversible capacity is at its highest, equalling 536 mA h g^{-1}.

Treatment with phosphoric acid can affect the physical and electrochemical properties of carbons made from melamine resin. At low temperature (600 °C), the introduction of phosphoric acid results in incomplete carbonization and the reversible capacity decreases with the amount of added phosphorus, especially below 0.9 V. At higher temperature (800 °C), the phosphoric acid introduced does not affect the carbonization significantly, and results in an increase of relative content of graphene nitrogen. The doped phosphorus exists as C—P—O in the carbon bulk and expands the layer places at the surface and in the graphite crystallites. Consequently, the intercalation of lithium is favoured, as is the reversible capacity, especially that above 0.9 V.

Dr. W. Maxwell is gratefully appreciated for help in the course of this work and the China Natural Sciences Foundation Committee is thanked for supplying partial funding for this work.

References

1 M. Nishijima, T. Kagohashi, M. Imanishi, Y. Takeda, O. Yamamoto and S. Kondo, *Solid State Ionics*, 1996, **83**, 107.
2 T. Shidai, S. Okada, S. Tobishima and J. Yamaki, *Solid State Ionics*, 1996, **86–88**, 785.
3 Y. Idota, T. Kubota, A. Matsufuji, Y. Maekawa and T. Miyasaka, *Science*, 1997, **276**, 1395.
4 I. A. Courtney and J. R. Dhan, *J. Electrochem. Soc.*, 1997, **144**, 2045.
5 Y. Nishi, *Kagaku Kogaku*, 1997, **61**, 424.
6 B. M. Way and J. R. Dhan, *J. Electrochem. Soc.*, 1994, **141**, 907.
7 A. M. Wilson and J. R. Dhan, *J. Electrochem. Soc.*, 1995, **142**, 366.
8 W. J. Weydanz, B. M. Way, T. van Buuren and J. R. Dhan, *J. Electrochem. Soc.*, 1994, **141**, 900.
9 S. Ito, T. Murata, M. Hasegawa, Y. Bito and Y. Toyoguchi, *Denki Kagaku*, 1996, **64**, 1180.
10 Y. P. Wu, S. B. Fang and Y. Y. Jiang, *Solid State Ionics*, in press.
11 X. Song, X. Chu and K. Kinoshita, *Mater. Res. Soc. Symp. Proc.*, 1995, **393**, 321.
12 Y. P. Wu, S. B. Fang, W. G. Ju and Y. Y. Jiang, *J. Power Sources*, 1998, **70**, 114.
13 Y. P. Wu, S. B. Fang and Y. Y. Jiang, *J. Power Sources*, 1998, **75**, 170.
14 A. Omura, H. Azuma, M. Aoki, A. Kita and Y. Nishi, in *Proceedings of the Symposium on Lithium Batteries*, ed. S. Surampudi and V. R. Koch, PV93-24, the Electrochemical Society Proceedings Series, Pennington, NJ, 1993, p. 21.
15 T. D. Tran, J. H. Feikert, X. Song and K. Kinoshita, *J. Electrochem. Soc.*, 1995, **142**, 3297.
16 J. Pisco and B. E. Warren, *J. Appl. Phys.*, 1942, **13**, 364.
17 B. Huang, Y. Huang, Z. Wang, L. Chen, R. Xue and F. Wang, *J. Power Sources*, 1996, **58**, 231.
18 A. Mabuchi, T. Katsuhisa, H. Fujimoto and T. Kasuh, *J. Electrochem. Soc.*, 1995, **142**, 1041.
19 S. Boses and R. H. Bragg, *Carbon*, 1981, **19**, 289.
20 K. J. Masters and B. McEnency, *Ext. Abstr. Program.-Bienn. Conf. Carbon*, 1979, **14**, 5.
21 G. Sandi, R. E. Winans and K. A. Carrado, *J. Electrochem. Soc.*, 1996, **143**, L95.
22 J. R. Dhan, T. Zheng, Y. Liu and J. S. Xue, *Science*, 1994, **264**, 556.
23 E. Peled, C. Menachem, D. Bar-Tow and A. Melman, *J. Electrochem. Soc.*, 1996, **143**, L4.
24 H. Ago, K. Tanaka, T. Yamabe, K. Takegoshi, T. Terao, S. Yata, Y. Hato and N. Ando, *Synth. Met.*, 1997, **89**, 141.
25 J. Laine, A. Calafat and M. Labady, *Carbon*, 1989, **27**, 191.
26 S. Oh and N. Rodriquez, *J. Mater. Res.*, 1993, **8**, 2879.

Paper 8/05080E